Copyright 2011 IEEE

Low-Complexity ICI/ISI Equalization in Doubly Dispersive Multicarrier Systems Using a Decision-Feedback LSQR Algorithm

Georg Tauböck, Mario Hampejs, Pavol Švač, Gerald Matz, Franz Hlawatsch, and Karlheinz Gröchenig

***Abstract*—We propose a low-complexity intercarrier interference/intersymbol interference (ICI/ISI) equalizer for multicarrier transmissions over doubly dispersive channels. Decision-feedback (or interference cancelation) is used with respect to both time and frequency. The ICI stage employs an extension of the iterative LSQR algorithm using groupwise interference cancelation with reliability-based sorting of sets of subcarriers and a band approximation of the frequency-domain channel matrix. The LSQR algorithm is attractive because of its excellent numerical properties and low complexity. Optimal pulse design is optionally considered for shaping the ICI/ISI. Simulation results demonstrate the excellent performance of the proposed ICI/ISI equalizer.**

***Index Terms*—Doubly dispersive channel, interference cancelation, intersymbol/intercarrier interference, LSQR algorithm, OFDM, pulse-shaping multicarrier transmission.**

I. Introduction

Orthogonal frequency-division multiplexing (OFDM) has recently been studied in scenarios with rapid channel variations, i.e., large Doppler frequency shifts; examples include Flash-OFDM [1], mobile reception of DVB-T [2], and base station cooperation in LTE [3]. The substantial intercarrier interference (ICI) resulting from large Doppler shifts [4]–[6] can be reduced via pulse shaping [6]–[12]. To mitigate the remaining ICI, various frequency-domain equalization methods have been proposed, including zero-forcing (ZF) and minimum mean-square error (MMSE) schemes [13]–[16], successive interference cancelation (SIC) [16]–[18], parallel interference cancelation (PIC) [2], [14], [15], [19], and hybrid SIC/PIC methods using groupwise interference cancelation (GIC) [20], [21]. In all schemes, equalizer complexity can be reduced by exploiting the (approximate) band structure of the frequency-domain channel matrix [5], [22]. The band approximation can be improved by pulse shaping [12] or time-domain windowing [23], [24].

The ICI equalizer in [25] applies the *LSQR algorithm* [26] in the time domain. LSQR is an iterative least-squares solver that has excellent numerical properties, can regularize the channel inversion by early termination of the iterations, and achieves low complexity by exploiting matrix sparsity (in [25], the band structure of the time-domain channel matrix). Since the complexity of the ICI equalizer in [25] scales with the maximum channel delay, it is attractive for channels with moderate delay spread.

In this correspondence, we focus on large delay spreads as, e.g., in single-frequency DVB-T networks. Here, a band approximation in the frequency domain is more efficient than in the time domain. Hence, we propose a *frequency-domain LSQR equalizer* as well as a "sequential" extension that we term the *S-LSQR algorithm* [27], [28]. S-LSQR employs a multi-recursion extension of *selective PIC* (SPIC) [29], in which a subset of "reliable" subcarriers is detected and canceled at each recursion. A similar strategy with a different reliability criterion and not using LSQR was previously proposed in [20] and [21]. For situations where intersymbol interference (ISI) occurs in addition to ICI, we combine the S-LSQR ICI equalizer with a temporal decision-feedback equalizer (DFE) structure. (For DFEs in OFDM, see also [30] and [31].)

The remainder of this correspondence is organized as follows. In Section II, we present the system model, discuss ICI and ISI, and review a method for pulse design. In Section III, we describe the proposed ICI/ISI equalization methods. Finally, simulation results are provided in Section IV.

II. System Model, ICI/ISI, and Pulse Design

We consider the discrete-time baseband representation of a pulse-shaping multicarrier system [6], [9], [12] with K subcarriers; symbol period $N \geq K$; complex data symbols $a_{l,k}$ with $l \in \mathbb{Z}$, $k \in \{0,\dots,K-1\}$ taken from some symbol alphabet $\mathcal{A}$, with $\mathrm{E}\{|a_{l,k}|^2\} = P_a$; transmit pulse $g(n)$ supported on $\{0,\dots,L_g-1\}$; and receive pulse $\gamma(n)$ supported on $\{0,\dots,L_\gamma-1\}$. A conventional OFDM system is obtained if $g(n)$ and $\gamma(n)$ are rectangular pulses supported on $\{K-N,\dots,K-1\}$ and $\{0,\dots,K-1\}$, respectively. We assume a doubly dispersive channel with impulse response $h(n,m)$ (maximum delay M) and white noise $z(n)$ of variance σ_z^2. The vector of demodulated symbols at symbol time l, $\mathbf{x}_l \triangleq (x_{l,0}\cdots x_{l,K-1})^T$, is related to the vectors of transmit symbols, $\mathbf{a}_{l'} \triangleq (a_{l',0}\cdots a_{l',K-1})^T$, as [9]

$$\mathbf{x}_l = \sum_{\lambda=-\infty}^{\infty} \mathbf{H}_{l,\lambda}\mathbf{a}_{l-\lambda} + \mathbf{z}_l, \qquad l \in \mathbb{Z}. \tag{1}$$

Here, the *frequency-domain channel matrices* $\mathbf{H}_{l,\lambda}$ of size $K \times K$ depend on $h(n,m)$, $g(n)$, and $\gamma(n)$ [9]. Furthermore, $\mathbf{z}_l \triangleq (z_{l,0}\cdots z_{l,K-1})^T$ with noise coefficients $z_{l,k}$ of variance $\sigma_{\mathrm{N}}^2 \triangleq \sigma_z^2 \sum_{n=0}^{L_\gamma-1} |\gamma(n)|^2$. For our discussion of ICI/ISI statistics and pulse design, we assume that the channel conforms to the wide-sense stationary uncorrelated scattering (WSSUS) model [32], with a scattering function that is supported in the rectangular delay-Doppler region $\{0,\dots,M\} \times [-\xi_{\max}, \xi_{\max}]$.

The (pure) ICI is described by the off-diagonal entries of the matrices $\mathbf{H}_{l,0}$, which were shown in [6], [33] to decay with growing distance from the main diagonal. Consider the mean power of an arbitrary entry on the κth diagonal, $P(\kappa) \triangleq \mathrm{E}\{|(\mathbf{H}_{l,0})_{0,\kappa}|^2\}$. The decay of $P(\kappa)$ with growing $|\kappa|$ motivates the approximation of $\mathbf{H}_{l,0}$ by a *(quasi-)banded matrix* $\widetilde{\mathbf{H}}_{l,0}$ given by $(\widetilde{\mathbf{H}}_{l,0})_{k,k'} \triangleq (\mathbf{H}_{l,0})_{k,k'}$ for $|k'-k| \leq B$ or $|k'-k| \geq K-B$ and $(\widetilde{\mathbf{H}}_{l,0})_{k,k'} \triangleq 0$ otherwise [12]. The ISI is described by all channel matrices $\mathbf{H}_{l,\lambda}$ for $\lambda \neq 0$; it consists of *postcursor* ISI ($\lambda > 0$) and *precursor* ISI ($\lambda < 0$). The matrices $\mathbf{H}_{l,\lambda}$ may only be nonzero for $-L_{\mathrm{pre}} \leq \lambda \leq L_{\mathrm{post}}$, with $L_{\mathrm{pre}} =$

Manuscript received August 08, 2010; revised November 24, 2010; accepted January 11, 2011. Date of publication February 10, 2011; date of current version April 13, 2011. The associate editor coordinating the review of this manuscript and approving it for publication was Prof. Ye (Geoffrey) Li. This work was supported by the FWF under Grants S10602, S10603, and S10606 within the National Research Network SISE and by the WWTF under Grants MA 44 (MOHAWI) and MA 07-004 (SPORTS). This work was presented in part at the IEEE Conference on Signal Processing Advances in Wireless Communications (SPAWC), Helsinki, Finland, June 2007, and IEEE SPAWC, Perugia, Italy, June 2009.

G. Tauböck, P. Švač, G. Matz, and F. Hlawatsch are with the Institute of Telecommunications, Vienna University of Technology, A-1040 Vienna, Austria (e-mail: gtauboec@nt.tuwien.ac.at; psvac@nt.tuwien.ac.at; gerald.matz@tuwien.ac.at; franz.hlawatsch@tuwien.ac.at).

M. Hampejs and K. Gröchenig are with the Numerical Harmonic Analysis Group, Faculty of Mathematics, University of Vienna, A-1090 Vienna, Austria (e-mail: mario.hampejs@univie.ac.at; karlheinz.groechenig@univie.ac.at).

Color versions of one or more of the figures in this correspondence are available online at http://ieeexplore.ieee.org.

Digital Object Identifier 10.1109/TSP.2011.2113181

1053-587X/$26.00 © 2011 IEEE

$\lfloor (L_\gamma - 1)/N \rfloor$ and $L_{\rm post} = \lfloor (L_g + M - 1)/N \rfloor$. A quasi-banded matrix approximation can also be used for $\mathbf{H}_{l,\lambda}$ when $\lambda \neq 0$. For the special case of OFDM, ISI is totally avoided if $M \leq N - K$.

An appropriate design of the pulses $g(n)$ and $\gamma(n)$ is helpful for shaping the ICI/ISI in a way consistent with the equalizer used. Following [6] and [12], we will design $g(n)$ and $\gamma(n)$ such that they maximize the "relevant signal-to-interference-plus-noise ratio"

$$J_{g,\gamma}(\lambda_0, \kappa_0) \triangleq \frac{P_a P(0)}{P_a \sigma_{\rm I}^2(\lambda_0, \kappa_0) + \sigma_{\rm N}^2},$$

with

$$P(0) = \mathrm{E}\left\{ |(\mathbf{H}_{l,0})_{0,0}|^2 \right\}$$

and

$$\sigma_{\rm I}^2(\lambda_0, \kappa_0) \triangleq \sum_{(\lambda,\kappa) \in \mathcal{I}(\lambda_0,\kappa_0)} \mathrm{E}\{ |(\mathbf{H}_{l,\lambda})_{0,\kappa}|^2 \}$$

where $\lambda_0 \in \{0, \ldots, L_{\rm post}\}$ and $\kappa_0 \in \{1, \ldots, B+1\}$. Here, the "relevant interference region" $\mathcal{I}(\lambda_0, \kappa_0)$ contains all index pairs (λ, κ) with $-L_{\rm pre} \leq \lambda \leq \lambda_0$ and $0 \leq \kappa \leq K-1$, except that for $\lambda = 0$, κ is restricted as $\kappa_0 \leq \kappa \leq K - \kappa_0$. The maximization of $J_{g,\gamma}(\lambda_0, \kappa_0)$ is carried out by means of a numerical optimization routine. The choice of λ_0 and κ_0 depends on the type of equalization used. If the equalizer employs a DFE for (postcursor) ISI cancelation, we set $\lambda_0 = 0$; here, only the precursor ISI is penalized by $J_{g,\gamma}(\lambda_0, \kappa_0)$. If no DFE is used, we set $\lambda_0 = L_{\rm post}$; here, the total ISI is penalized [12]. Similarly, for an ICI equalizer using a banded-matrix approximation with bandwidth B, we set $\kappa_0 = B + 1$; here, only the ICI outside the matrix band (corresponding to $B+1 \leq \kappa \leq K - B - 1$) is penalized. In contrast, for $\kappa_0 = 1$, the total ICI is penalized.

III. ICI/ISI Equalization

A. ISI Equalization

For rapid channel variations, it is no longer feasible to use classical OFDM techniques to cope with large channel delays. Indeed, an increase of the cyclic prefix length or the number of subcarriers (for a fixed transmit bandwidth) would result in even larger channel variations within one OFDM symbol period and, hence, in increased ICI; furthermore, the design of time-domain (channel shortening) equalizers has so far been limited to time-invariant channels. For this reason, we here pursue an ISI mitigation strategy consisting of an appropriate pulse design and the use of a DFE. When the channel delays are large, mitigating the *total* ISI by a pulse design with $\lambda_0 = L_{\rm post}$ as explained in Section II has been observed to lead to very short pulses, which tend to result in poor ICI equalization performance (see Section IV-B). Therefore, it may be preferable to minimize only the precursor ISI by the pulse design (using $\lambda_0 = 0$) and to cancel the postcursor ISI by means of a DFE [30], [31].

In the DFE, a replica of the postcursor ISI is generated from the $L_{\rm post}$ previously detected symbol vectors $\hat{\mathbf{a}}_{l-\lambda}, \lambda = 1, \ldots, L_{\rm post}$ and subtracted from the received (demodulated) signal $\mathbf{x}_l$:

$$\mathbf{y}_l \triangleq \mathbf{x}_l - \sum_{\lambda=1}^{L_{\rm post}} \widetilde{\mathbf{H}}_{l,\lambda} \hat{\mathbf{a}}_{l-\lambda}. \tag{2}$$

Here, $\hat{\mathbf{a}}_l \in \mathcal{A}^K$ denotes the detected (quantized) symbol vector at time l and $\widetilde{\mathbf{H}}_{l,\lambda}$ is the quasi-banded approximation to $\mathbf{H}_{l,\lambda}$, which is used to reduce the complexity of computing (2). Inserting (1) in (2) while assuming correct symbol detection (i.e., $\hat{\mathbf{a}}_l = \mathbf{a}_l$), we obtain $\mathbf{y}_l = \widetilde{\mathbf{H}}_{l,0} \mathbf{a}_l + \tilde{\mathbf{z}}_l$. Here, by definition, $\tilde{\mathbf{z}}_l$ contains the noise $\mathbf{z}_l$, residual precursor ISI due to imperfect pulse design, residual postcursor ISI due to the quasi-banded approximation in (2), and ICI not accounted for by $\widetilde{\mathbf{H}}_{l,0}$. In what follows, we will consider a fixed symbol time l and briefly write the above relation as $\mathbf{y} = \widetilde{\mathbf{H}}\mathbf{a} + \tilde{\mathbf{z}}$.

B. ICI Equalization Based on the LSQR Algorithm

The vector $\mathbf{y} = \widetilde{\mathbf{H}}\mathbf{a} + \tilde{\mathbf{z}}$ forms the input to the ICI equalizer. The proposed ICI equalizers use the quasi-banded approximation $\widetilde{\mathbf{H}}$ and the LSQR algorithm [26], [27], [34]. LSQR is an iterative procedure for solving large, sparse, possibly ill-conditioned least-squares (LS) problems. In our case, the LS problem is given by $\min_{\mathbf{a} \in \mathbb{C}^K} \|\mathbf{y} - \widetilde{\mathbf{H}}\mathbf{a}\|^2$, which is equivalent to the normal equations $\widetilde{\mathbf{H}}^H \widetilde{\mathbf{H}} \mathbf{a} = \widetilde{\mathbf{H}}^H \mathbf{y}$ [35]. The LSQR algorithm has very low complexity in our context because it is tailored to sparse matrices [26] such as our quasi-banded channel matrix $\widetilde{\mathbf{H}}$. Furthermore, it achieves a regularization of the notoriously ill-conditioned channel matrix $\widetilde{\mathbf{H}}$ simply by an early termination of the iterations [34]. Finally, memory requirements are low due to a recursive implementation discussed in [26].

In exact arithmetic, the LSQR algorithm is equivalent to a method known as *conjugate gradient on the normal equations* (CGNE). However, in fixed-point arithmetic, it has a lower complexity and better numerical stability than CGNE. In the ith LSQR iteration, an approximate solution to the normal equations is obtained by minimizing $\|\mathbf{y} - \widetilde{\mathbf{H}}\mathbf{a}\|$ subject to the constraint that $\mathbf{a}$ lies in the Krylov subspace[1] $\mathcal{K}(\widetilde{\mathbf{H}}^H \widetilde{\mathbf{H}}, \widetilde{\mathbf{H}}^H \mathbf{y}, i)$. A regularization is achieved through an early termination of the iterations [34], because the initial iterations reduce the approximation error $\|\mathbf{y} - \widetilde{\mathbf{H}}\mathbf{a}\|$ in the directions of the dominant right singular vectors of $\widetilde{\mathbf{H}}$, which are least affected by noise. The optimum number of iterations corresponds to maximum ICI mitigation and minimum noise enhancement and is usually unkown. Fortunately, moderate deviations from the optimum number of iterations do not degrade the performance significantly. The complexity order of the LSQR algorithm is $\mathcal{O}(K(2B+1)I)$ operations, where I denotes the number of iterations used. Thus, the complexity is linear in the number of subcarriers K, the matrix bandwidth B, and the number of iterations I.

C. ICI Equalization Based on the S-LSQR Algorithm

Next, we propose a "sequential" version of the LSQR equalizer, termed the *S-LSQR equalizer*, which incorporates a multi-recursion extension of SPIC [29]. This interference cancelation algorithm differs from SPIC in that it uses several recursions to detect and cancel the symbols. In each recursion, the symbols are divided into reliable and unreliable symbols based on a *dynamic* threshold comparison. Except for the reliability criterion, this is similar to *modified SIC* [20], [21], which cancels the contribution of a subset of symbols with the highest signal-to-noise ratio (SNR) in each recursion. (We do not use the SNR-based criterion in the S-LSQR equalizer because, due to the iterative nature of LSQR, a closed-form expression of the post-equalization SNRs of the various subcarriers is not available.)

In the rth recursion ($r \geq 2$), the input to the S-LSQR equalizer is given by the "reduced vector" $\mathbf{y}^{(r-1)} \in \mathbb{C}^K$ and the previously detected symbol vectors $\hat{\boldsymbol{\alpha}}^{(1)}, \ldots, \hat{\boldsymbol{\alpha}}^{(r-1)}$ of respective dimensions $J_1, \ldots, J_{r-1}$. In the absence of detection errors, $\mathbf{y}^{(r-1)}$ corresponds to the reduced system model $\mathbf{y}^{(r-1)} = \widetilde{\mathbf{H}}^{(r-1)} \mathbf{a}^{(r)} + \tilde{\mathbf{z}}$. Here, $\mathbf{a}^{(r)} \in \mathcal{A}^{K - J_1 - \cdots - J_{r-1}}$ is the vector of all transmit symbols in $\mathbf{a}$ except those corresponding to $\hat{\boldsymbol{\alpha}}^{(1)}, \ldots, \hat{\boldsymbol{\alpha}}^{(r-1)}$, and the $K \times (K - J_1 - \cdots - J_{r-1})$ matrix $\widetilde{\mathbf{H}}^{(r-1)}$ contains the corresponding columns of $\widetilde{\mathbf{H}}$.

[1]The Krylov subspace $\mathcal{K}(\mathbf{A}, \mathbf{b}, i)$ is the space spanned by the $i+1$ vectors $\mathbf{b}, \mathbf{A}\mathbf{b}, \ldots, \mathbf{A}^i \mathbf{b}$ [36, Sec. 9.1.1].

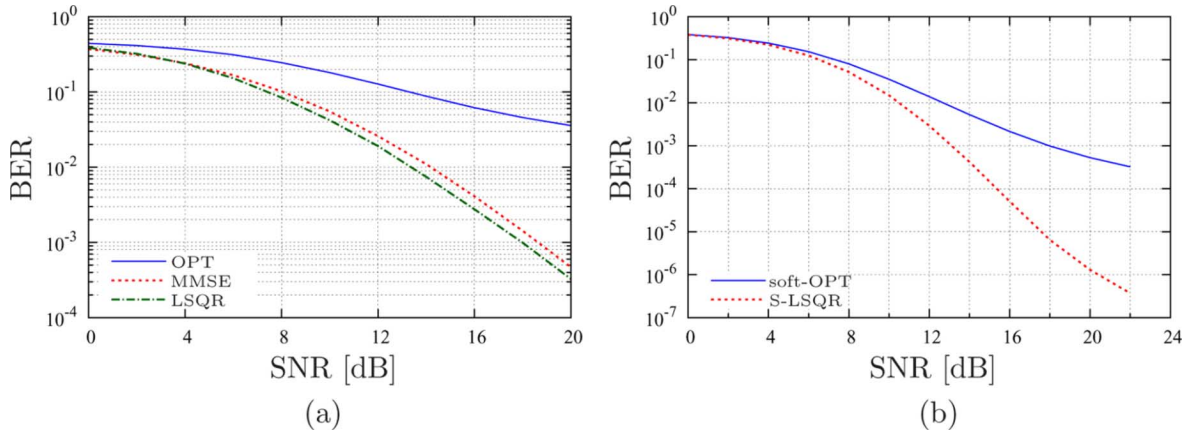

Fig. 1. BER of various ICI equalizers versus SNR: (a) comparison of LSQR, MMSE, and OPT, (b) comparison of S-LSQR and soft-decision OPT.

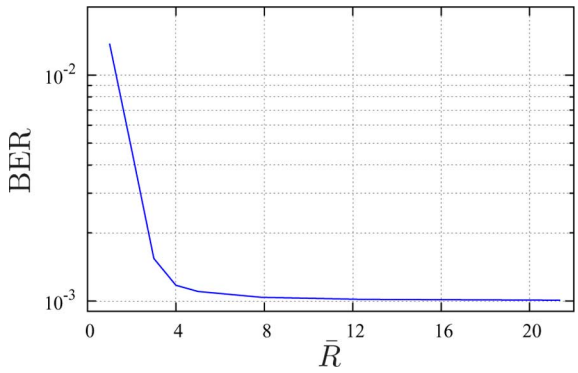

Fig. 2. BER of S-LSQR versus mean number $\bar{R}$ of S-LSQR recursions for SNR $= 12$ dB.

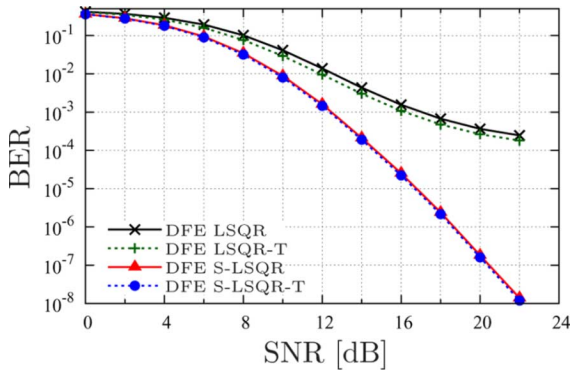

Fig. 3. BER of various ICI/ISI equalizers versus SNR.

First, the basic LSQR equalizer is applied to $\mathbf{y}^{(r-1)}$, using $\widetilde{\mathbf{H}}^{(r-1)}$ as the system matrix. Let $\hat{\mathbf{a}}^{(r)} \in \mathbb{C}^{K-J_1-\cdots-J_{r-1}}$ denote the resulting symbol vector estimate; $\hat{\mathbf{a}}^{(r)} \in \mathcal{A}^{K-J_1-\cdots-J_{r-1}}$ the quantized version of $\tilde{\mathbf{a}}^{(r)}$; and $\hat{\boldsymbol{\alpha}}^{(r)} \in \mathcal{A}^{J_r}$ the subvector of $\hat{\mathbf{a}}^{(r)}$ that contains all quantized symbols satisfying the reliability criterion defined below. In the subsequent interference cancelation step, the reduced vector $\mathbf{y}^{(r)} \triangleq \mathbf{y}^{(r-1)} - \mathbf{G}^{(r)}\hat{\boldsymbol{\alpha}}^{(r)}$ is calculated, where $\mathbf{G}^{(r)}$ is formed by the J_r columns of $\widetilde{\mathbf{H}}$ corresponding to the symbols in $\hat{\boldsymbol{\alpha}}^{(r)}$. If the detected symbols $\hat{\boldsymbol{\alpha}}^{(r)}$ are correct, $\mathbf{y}^{(r)}$ corresponds to the reduced system model

$$\mathbf{y}^{(r)} = \widetilde{\mathbf{H}}^{(r)}\mathbf{a}^{(r+1)} + \tilde{\mathbf{z}} \tag{3}$$

where $\mathbf{a}^{(r+1)} \in \mathcal{A}^{K-J_1-\cdots-J_r}$ contains all transmit symbols except those corresponding to $\hat{\boldsymbol{\alpha}}^{(1)}, \ldots, \hat{\boldsymbol{\alpha}}^{(r)}$ and $\widetilde{\mathbf{H}}^{(r)}$ contains the corresponding columns of $\widetilde{\mathbf{H}}$. Thus, (3) no longer contains the $J_1 + \cdots + J_r$ symbols corresponding to $\hat{\boldsymbol{\alpha}}^{(1)}, \ldots, \hat{\boldsymbol{\alpha}}^{(r)}$.

This recursive procedure is initialized at $r = 1$ by applying the basic LSQR equalizer to the ICI equalizer input $\mathbf{y} = \widetilde{\mathbf{H}}\mathbf{a} + \tilde{\mathbf{z}}$. Note that error propagation is minimized by subtracting the contribution of the *most reliably* detected symbols in each recursion. This improves on previously proposed iterative ICI equalization schemes without reliability-based sorting [23].

We now describe our dynamic reliability criterion for a 2^{2m}-QAM constellation[2]

$$\mathcal{A} = \{a = a_{\mathrm{R}} + ja_{\mathrm{I}} : a_{\mathrm{R}}, a_{\mathrm{I}} \in \{\pm 1, \pm 3, \ldots, \pm(2^m - 1)\}\}$$

[2]A similar criterion for, e.g., PSK constellations can be formulated in a straightforward manner.

where $m \in \{1, 2, \ldots\}$. Inspired by [29] and [37], for each QAM symbol coordinate $\eta \in \{\pm 1, \pm 3, \ldots, \pm(2^m - 1)\}$, we define a *reliability interval* $\mathcal{I}_r(\eta)$ in the rth S-LSQR recursion as follows: $\mathcal{I}_r(\eta) = [\eta - T_r^{(i)}, \eta + T_r^{(i)}]$ for $\eta \in \{\pm 1, \pm 3, \ldots, \pm(2^m - 3)\}$ (inner symbols); $\mathcal{I}_r(\eta) = [\eta - T_r^{(o)}, \infty)$ for $\eta = (2^m - 1)$ and $\mathcal{I}_r(\eta) = (-\infty, \eta + T_r^{(o)}]$ for $\eta = -(2^m - 1)$ (outer symbols), where $0 < T_r^{(i)} < 1$ and $T_r^{(o)} \leq 1$. Then, for each symbol $a = a_{\mathrm{R}} + ja_{\mathrm{I}} \in \mathcal{A}$, we define a *reliability region* (RR) as $\mathcal{R}_r(a) \triangleq \mathcal{I}_r(a_{\mathrm{R}}) \times \mathcal{I}_r(a_{\mathrm{I}})$. In each recursion of the S-LSQR equalizer, a quantized symbol $\hat{a}$ is classified as *reliable* if the corresponding equalized symbol before quantization $\tilde{a}$ is located in one of the RRs. The resulting reliability-based decision scheme is intermediate between soft and hard, but much less computationally demanding than soft interference cancelation. Because the interference tends to decrease after each recursion, we set $T_{r+1}^{(i)} = T_r^{(i)} + \epsilon$ and $T_{r+1}^{(o)} = T_r^{(o)} + \epsilon$ with a predefined ε; this results in a reduction of the number of recursions required.

The complexity of the S-LSQR equalizer is upper bounded by $\mathcal{O}(K(2B + 1)IR)$, where I is the number of LSQR iterations performed in each S-LSQR recursion (here assumed equal in all S-LSQR recursions for simplicity) and R is the number of S-LSQR recursions. Clearly, R depends on the thresholds $T_r^{(i)}$ and $T_r^{(o)}$, which in turn determine the performance of the S-LSQR equalizer. Minimum complexity ($R = 1$) is obtained for $T_1^{(i)} = 1$ and $T_1^{(o)} = 1$, in which case the S-LSQR equalizer reduces to the LSQR equalizer with complexity $\mathcal{O}(K(2B + 1)I)$. At the other extreme, the best performance is obtained by processing only a single symbol in each recursion; here, we obtain $R = K$ and thus the complexity becomes $\mathcal{O}(K^2(2B+1)I)$. In general, processing fewer symbols per recursion

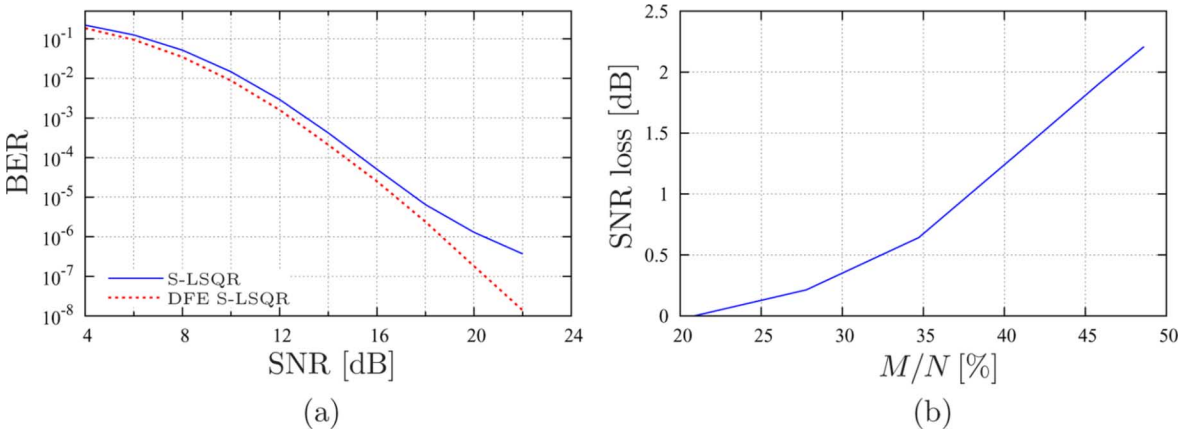

Fig. 4. Comparison of S-LSQR (with non-DFE pulses) and DFE S-LSQR (with DFE pulses): (a) BER versus SNR, (b) SNR loss of S-LSQR relative to DFE S-LSQR versus M/N, at $\mathrm{BER} = 10^{-3}$.

and, hence, using more recursions results in a higher complexity but also in a better performance (see Section IV-A).

IV. Simulation Results

We simulated a pulse-shaping multicarrier system with $K = 128$ subcarriers and symbol period $N = 144$, using a rate-1/2 convolutional code, a 16×16 row-column interleaver, and a 4-QAM symbol alphabet. A WSSUS channel with brick-shaped scattering function was generated according to [38] using maximum channel delay $M = 50$ (except in Fig. 4(b)) and maximum normalized Doppler frequency $\xi_{\max} = 10^{-3}$ (this corresponds to a maximum Doppler frequency of 12.8% of the subcarrier frequency spacing and an rms Doppler spread of 7.4% of the subcarrier frequency spacing). The channel matrix bandwidth used for pulse design and for equalization was chosen as $B = 10$. The pulses were optimized numerically, formally using $\sigma_{\mathrm{N}}^2 = 0$ regardless of the true SNR. The DFE length resulted as $L_{\mathrm{post}} = 1$ for all M. The (S-)LSQR algorithm performed $I = 16$ LSQR iterations unless stated otherwise. The threshold parameter was initially set to $T_1^{(o)} = -0.4$ (i.e., initially the symbols were not contained in the respective RRs) and increased by a fixed ε ($= 0.2$ except in Fig. 2) at the end of each S-LSQR recursion; this resulted in at most $R = 8$ recursions.

A. Performance Comparison of (S-)LSQR, MMSE, and OPT

We first compare the proposed LSQR-based ICI equalizer—without recursive ICI cancelation—with (i) an MMSE equalizer [16] and (ii) an equalizer using the operator perturbation technique (OPT) [15] combined with first-order Auer acceleration [15], [39], both using a quasi-banded channel matrix. The pulses were designed using $\lambda_0 = L_{\mathrm{post}} = 1$ and $\kappa_0 = B+1 = 11$. Fig. 1(a) shows the coded bit-error rate (BER) of the three ICI equalizers versus the SNR. The number of LSQR iterations was chosen small ($I = 10$) for low SNR (0–10 dB) to obtain a stronger implicit regularization, and larger for medium and high SNR ($I = 16$ for 12–18 dB; $I = 30$ for 20 dB) to improve the accuracy of the approximate matrix inversion. It is seen that LSQR performs significantly better than OPT (which has convergence problems due to the insufficient diagonal dominance of the channel matrix [40]), similar to MMSE for small SNR, and slightly better than MMSE for SNR higher than about 6 dB. In Fig. 1(b), we compare S-LSQR and OPT. For a fair comparison of these two cancelation schemes, we employ soft-decisions within the OPT (PIC) scheme [15], which become harder with progressing iterations. This is similar in spirit to the dynamic choice of the threshold made by S-LSQR (see Section III-C). It is seen that S-LSQR outperforms soft-decision OPT for medium and high SNR.

Fig. 2 shows the BER obtained with S-LSQR versus the mean number of S-LSQR recursions (denoted $\bar{R}$), for $\mathrm{SNR} = 12$ dB and $T_1^{(o)} = -0.4$. We chose different values of ε and, for each ε, performed 5000 simulation runs and calculated $\bar{R}$ and the BER. It is seen that, as $\bar{R}$ increases, the BER drops quickly initially but then levels off after about $\bar{R} = 4$. Hence, the performance gain of S-LSQR (relative to LSQR) is achieved already with a small number of recursions.

B. Performance Comparison of DFE S-LSQR, DFE LSQR, and S-LSQR

Next, we include ISI mitigation. Fig. 3 shows the BER of DFEs with LSQR-based and S-LSQR-based ICI equalization (abbreviated DFE LSQR and DFE S-LSQR). To analyze error propagation in the DFE, we also consider genie-aided feedback of the true symbols (abbreviated DFE LSQR-T and DFE S-LSQR-T). It is seen that DFE S-LSQR significantly outperforms DFE LSQR, especially at medium to high SNR. Thus, the generalized SPIC used by DFE S-LSQR is effective in combating the various impairments (ICI, residual ISI, band approximation error). Furthermore, error propagation is seen to be negligible. This can be explained by the following two facts. First, we use a vector DFE (the vector being defined by the subcarriers), and a few incorrectly detected subcarrier symbols have a rather limited effect on the postcursor ISI cancelation. Second, even if error propagation occurs on a few subcarriers, the subsequent code (which operates across the subcarriers) is typically able to correct the erroneous bits.

Finally, Fig. 4(a) compares two approaches to mitigating ISI: i) pure ICI equalization using S-LSQR, with pulses minimizing both precursor and postcursor ISI ("non-DFE pulses"), and ii) combined ICI/ISI equalization using DFE S-LSQR, with pulses minimizing only the precursor ISI ("DFE pulses"). It is seen that DFE S-LSQR outperforms S-LSQR. Additional simulations suggest that this is caused by a higher condition number of $\widetilde{\mathbf{H}}$ obtained for the non-DFE pulses. In Fig. 4(b), we display the SNR loss of S-LSQR relative to DFE S-LSQR at $\mathrm{BER} = 10^{-3}$ as a function of M; the non-DFE and DFE pulses were designed individually for each M. One can observe that DFE S-LSQR is advantageous over S-LSQR especially for highly time-dispersive channels (large M).

V. Conclusion

We proposed a low-complexity ICI/ISI equalizer for pulse-shaping multicarrier transmissions (including OFDM) that is especially suited for strongly time-frequency dispersive channels. At the heart of this equalizer is the use of the iterative LSQR algorithm for ICI mitigation in the frequency domain, combined with a band approximation of

the channel matrix. The LSQR algorithm is attractive because of its inherent regularization and low complexity. We augmented the LSQR algorithm by groupwise ICI cancelation with reliability-based sorting of subcarrier sets and a temporal decision-feedback structure for canceling the postcursor ISI. The precursor ISI can be minimized by a suitable (optimum) design of the transmit and receive pulses. Our simulation results demonstrated the excellent performance of the proposed ICI/ISI equalizer already for a small number of ICI cancelation recursions.

REFERENCES

[1] Flarion Technologies, "OFDM for mobile data communications," White Paper, 2003.

[2] S. Tomasin, A. Gorokhov, H. Yang, and J. P. Linnartz, "Iterative interference cancellation and channel estimation for mobile OFDM," *IEEE Trans. Wireless Comm.*, vol. 4, pp. 238–245, Jan. 2005.

[3] V. Kotzsch and G. Fettweis, "Interference analysis in time and frequency asynchronous network MIMO OFDM systems," in *Proc. IEEE Wireless Commun. Netw. Conf. (WCNC)*, Sidney, Australia, Apr. 2010.

[4] A. Stamoulis, S. N. Diggavi, and N. Al-Dhahir, "Intercarrier interference in MIMO OFDM," *IEEE Trans. Signal Process.*, vol. 50, no. 10, pp. 2451–2464, Oct. 2002.

[5] X. Cai and G. B. Giannakis, "Bounding performance and suppressing intercarrier interference in wireless mobile OFDM," *IEEE Trans. Commun.*, vol. 51, pp. 2047–2056, Dec. 2003.

[6] G. Matz, D. Schafhuber, K. Gröchenig, M. Hartmann, and F. Hlawatsch, "Analysis, optimization, and implementation of low-interference wireless multicarrier systems," *IEEE Trans. Wireless Comm.*, vol. 6, pp. 1921–1931, May 2007.

[7] A. Vahlin and N. Holte, "Optimal finite duration pulses for OFDM," *IEEE Trans. Commun.*, vol. 4, pp. 10–14, Jan. 1996.

[8] R. Haas and J. C. Belfiore, "A time-frequency well-localized pulse for multiple carrier transmission," *Wireless Personal Commun.*, vol. 5, pp. 1–18, 1997.

[9] W. Kozek and A. F. Molisch, "Nonorthogonal pulseshapes for multicarrier communications in doubly dispersive channels," *IEEE J. Sel. Areas Comm.*, vol. 16, pp. 1579–1589, Oct. 1998.

[10] H. Bölcskei, "Efficient design of pulse shaping filters for OFDM systems," in *Proc. SPIE Wavelet Appl. Signal Image Process. VII*, Denver, CO, Jul. 1999, pp. 625–636.

[11] T. Strohmer and S. Beaver, "Optimal OFDM design for time-frequency dispersive channels," *IEEE Trans. Commun.*, vol. 51, pp. 1111–1122, Jul. 2003.

[12] S. Das and P. Schniter, "Max-SINR ISI/ICI-shaping multicarrier communication over the doubly dispersive channel," *IEEE Trans. Signal Process.*, vol. 55, no. 12, pp. 5782–5795, Dec. 2007.

[13] W. G. Jeon, K. H. Chang, and Y. S. Cho, "An equalization technique for orthogonal frequency-division multiplexing systems in time-variant multipath channels," *IEEE Trans. Commun.*, vol. 47, no. 1, pp. 27–32, Jan. 1999.

[14] Q. Xuerong and Z. Lijun, "Interchannel interference cancellation in wireless OFDM systems via Gauss–Seidel method," in *Proc. IEEE Int. Conf. Commun. Technol. (ICCT)*, Beijing, China, Apr. 2003, vol. 2, pp. 1051–1055.

[15] A. F. Molisch, M. Toeltsch, and S. Vermani, "Iterative methods for cancellation of intercarrier interference in OFDM systems," *IEEE Trans. Veh. Technol.*, vol. 56, no. 4, pp. 2158–2167, 2007.

[16] Y.-S. Choi, P. J. Voltz, and F. A. Cassara, "On channel estimation and detection for multicarrier signals in fast and selective Rayleigh fading channels," *IEEE Trans. Commun.*, vol. 49, pp. 1375–1387, Aug. 2001.

[17] E. Leung and P. Ho, "A successive interference cancellation scheme for an ODFM system," in *Proc. IEEE Int. Conf. Commun. (ICC)*, Atlanta, GA, Jun. 1998, pp. 375–379.

[18] K. Kim and H. Park, "A low complexity ICI cancellation method for high mobility OFDM systems," in *Proc. IEEE Veh. Technol. Conf. (VTC)—Spring*, Melbourne, Australia, May 2006, pp. 2528–2532.

[19] A. Gorokhov and J.-P. Linnartz, "Robust OFDM receivers for dispersive time varying channels: Equalisation and channel acquisition," in *Proc. IEEE Int. Conf. Commun. (ICC)*, New York, Apr./May 2002, pp. 470–474.

[20] J. Cai, J. Mark, and X. Shen, "ICI cancellation in OFDM wireless communication systems," in *Proc. IEEE GLOBECOM*, Taipei, Taiwan, R.O.C., 2002, vol. 1, pp. 656–660.

[21] X. N. Tran and T. Fujino, "Groupwise successive ICI cancellation for OFDM systems in time-varying channels," in *Proc. IEEE Symp. Signal Process. Inf. Technol. (ISSPIT)*, Athens, Greece, Dec. 2005, pp. 489–494.

[22] L. Rugini, P. Banelli, and G. Leus, "Simple equalization of time-varying channels for OFDM," *IEEE Commun. Lett.*, vol. 9, pp. 619–621, Jul. 2005.

[23] P. Schniter, "Low-complexity equalization of OFDM in doubly-selective channels," *IEEE Trans. Signal Process.*, vol. 52, no. 4, pp. 1002–1011, Apr. 2004.

[24] L. Rugini, P. Banelli, and G. Leus, "Low-complexity banded equalizers for OFDM systems in Doppler spread channels," *EURASIP J. Appl. Signal Process.*, vol. 19, pp. 1–13, 2006.

[25] T. Hrycak and G. Matz, "Low-complexity time-domain ICI equalization for OFDM communications over rapidly varying channels," in *Proc. Asilomar Conf. Signals, Syst., Comput.*, Pacific Grove, CA, Oct. –Nov. 2006, pp. 1767–1771.

[26] C. C. Paige and M. A. Saunders, "LSQR: An algorithm for sparse linear equations and sparse least squares," *ACM Trans. Math. Softw.*, vol. 8, pp. 43–71, Mar. 1982.

[27] G. Tauböck, M. Hampejs, G. Matz, F. Hlawatsch, and K. Gröchenig, "LSQR-based ICI equalization for multicarrier communications in strongly dispersive and highly mobile environments," in *Proc. IEEE-SP Workshop Signal Process. Adv. Wireless Commun.*, Helsinki, Finland, Jun. 2007.

[28] M. Hampejs, P. Švač, G. Tauböck, K. Gröchenig, F. Hlawatsch, and G. Matz, "Sequential LSQR-based ICI equalization and decision-feedback ISI cancellation in pulse-shaped multicarrier systems," in *Proc. IEEE-SP Workshop Signal Process. Adv. Wireless Commun.*, Perugia, Italy, Jun. 2009.

[29] R. Fantacci, "Proposal of an interference cancellation receiver with low complexity for DS/CDMA mobile communication systems," *IEEE Trans. Veh. Technol.*, vol. 48, no. 4, pp. 1039–1046, 1999.

[30] Y. Sun, "Bandwidth-efficient wireless OFDM," *IEEE J. Sel. Areas Commun.*, vol. 19, no. 11, pp. 2267–2278, 2001.

[31] L. Rugini, P. Banelli, R. C. Cannizzaro, and G. Leus, "Channel estimation and windowed DFE for OFDM with Doppler spread," in *Proc. IEEE Int. Conf. Acoust., Speech, Signal Process. (ICASSP)*, Toulouse, France, May 2006, vol. IV, pp. 137–140.

[32] P. A. Bello, "Characterization of randomly time-variant linear channels," *IEEE Trans. Commun. Syst.*, vol. 11, no. 4, pp. 360–393, 1963.

[33] K. Gröchenig, "Time-frequency analysis of Sjöstrand's class," *Revista Mat. Iberoam.*, vol. 22, no. 2, pp. 703–724, 2006.

[34] P. C. Hansen, *Rank-Deficient and Discrete Ill-Posed Problems: Numerical Aspects of Linear Inversion*. Philadelphia, PA: SIAM, 1998.

[35] E. E. Osborne, "On least squares solutions of linear equations," *J. Assoc. Comput. Mach.*, vol. 8, pp. 628–636, 1961.

[36] G. H. Golub and C. F. Van Loan, *Matrix Computations*, 3rd ed. Baltimore, MD: The Johns Hopkins Univ. Press, 1996.

[37] M. Chiani, "Introducing erasures in decision-feedback equalization to reduce error propagation," *IEEE Trans. Commun.*, vol. 45, no. 7, pp. 757–760, 1997.

[38] D. Schafhuber, G. Matz, and F. Hlawatsch, "Simulation of wideband mobile radio channels using subsampled ARMA models and multistage interpolation," in *Proc. 11th IEEE Workshop Statist. Signal Process.*, Singapore, Aug. 2001, pp. 571–574.

[39] L. Auer, "Acceleration of convergence," in *Numerical Radiative Transfer*, W. Kalkofen, Ed. Cambridge, U.K.: Cambridge Univ. Press, 1987.

[40] C. T. Kelley, *Iterative Methods for Linear and Nonlinear Equations*. Philadelphia, PA: SIAM, 1995.